Pattern Recognition Letters 000 (2018) 1–8

Contents lists available at ScienceDirect

Pattern Recognition Letters

journal homepage: www.elsevier.com/locate/patrec

Robust rigid registration algorithm based on pointwise correspondence and correntropy

Shaoyi Du[a,*], Guanglin Xu[a], Sirui Zhang[b], Xuetao Zhang[a], Yue Gao[c], Badong Chen[a]

[a] Institute of Artificial Intelligence and Robotics, School of Electronic and Information Engineering, Xi'an Jiaotong University, Xi'an 710049, China
[b] School of Software Engineering, Xi'an Jiaotong University, Xi'an 710049, China
[c] School of Software, Tsinghua University, Beijing 100084, China

ARTICLE INFO

Article history:
Available online xxx

Keywords:
Iterative closest point (ICP)
Correntropy
Outliers
Noises
Rigid registration

ABSTRACT

The iterative closest point (ICP) algorithm is fast and accurate for rigid point set registration, but it works badly when handling noisy data or point clouds with outliers. This paper instead proposes a novel method based on the ICP algorithm to deal with this problem. Firstly, correntropy is introduced into the rigid registration problem which could handle noises and outliers well, and then a new energy function based on maximum correntropy criterion is proposed. After that, a new ICP algorithm based on correntropy is proposed, which performs well in dealing with rigid registration with noises and outliers. This new algorithm converges monotonically from any given parameters, which is similar to the ICP algorithm. Experimental results demonstrate its accuracy and robustness compared with the traditional ICP algorithm.

1. Introduction

With the rise of machine learning, many normalized image samples are required for training the models. Since that, image registration based on features is a useful method for aligning the samples, which is a preprocessing step for machine learning. Although there are many feature selection methods [1–3], the edge points of the images and the 3D point clouds representing the shapes of the objects are used as common features. Therefore, point set registration is a popular research issue in image classification [4,5], simulated mapping and localization (SLAM) [6,7], medical image analysis [8,9] and other engineering fields. The so-called point set registration, that is, two or more groups of the same or similar point sets undergo a space geometry transformation, so that the corresponding points can be aligned correctly. The iteration closest point (ICP) algorithm [10–12] is known to be employed to solve this problem because of its accuracy and efficiency.

Until now, more and more related works have been done for improving the speed and robustness of the ICP algorithm. Fitzgibbon [13] employed the Levenberg–Marquardt algorithm to speed up ICP, Sharp et al. [14] introduced invariant features to avoid the ICP algorithm being trapped into local minimum, and Blais et al. [15] employed a projection method to find the correspondence to speed up ICP. In addition, many researchers have studied point set registration with the outliers and noises. Chetverikov et al. [16] proposed the trimmed ICP (TrICP) algorithm for partially overlapping registration. Du et al. [17,18] proposed probability ICP for registration of point sets with noises. Granger et al. [19] proposed multi-scale EM-ICP algorithm which introduced the full correspondence relationships of all the points. Moreover, some scholars used the soft-assign method based on the full correspondence to tackle the registration with outliers and less noises, algorithms like TPS-RPM [20] and CPD [21] deal with registration in this way. The algorithms are all time-consuming and they are easily affected by the noises.

However, all above-mentioned works are based on Euclidean distance, which depends on the parameters greatly and cannot process the outliers and noises at the same time. It is well known that correntropy [22,23] can effectively deal with the outliers and noises, which is not sensitive to the parameters, so we propose a mathematical model based on correntropy. Then, we propose a new registration function based on maximum correntropy criterion (MCC), which is solved by a novel ICP algorithm. This algorithm is proved to be efficient and accurate in the experiments.

The rest of this paper is organized as follows. In Section 2, related works including ICP algorithm and correntropy are stated. In Section 3, an optimization model based on correntropy is proposed, and then the proposed method – the ICP algorithm based on MCC is given. Furthermore, the detailed analysis of the proposed algorithm is discussed in the next section. In Section 5, the experimental results are shown to demonstrate the accuracy

* Corresponding author.
E-mail address: dushaoyi@xjtu.edu.cn (S. Du).

https://doi.org/10.1016/j.patrec.2018.06.028
0167-8655/

and efficiency of our algorithm. In the last section, a conclusion is drawn finally.

2. Related work

2.1. ICP algorithm

In this part, we will take a brief review of the ICP algorithm. Given two point sets in $\mathbb{R}^n$, a data point set $X \triangleq \{\vec{x}_i\}_{i=1}^{N_x}$ $(N_x \in \mathbb{N})$ and a target point set $Y \triangleq \{\vec{y}_i\}_{i=1}^{N_y}$ $(N_y \in \mathbb{N})$. The goal of a rigid registration is to find a rotation matrix $\mathbf{R}$ and a translation vector $\vec{t}$, with which the data set X is in the best alignment with the target set Y. The least square (LS) problem based on Euclidean distance is formulated as follows:

$$\min_{\mathbf{R},\vec{t},c(i)\in\{1,2,\ldots,N_y\}} \sum_{i=1}^{N_x} ||(\mathbf{R}\vec{x}_i + \vec{t}) - \vec{y}_{c(i)}||_2^2 \quad (1)$$

$$s.t. \quad \mathbf{R}^T\mathbf{R} = \mathbf{I}_m, \quad \det(\mathbf{R}) = 1.$$

The ICP algorithm is proposed to solve this problem for its accuracy and efficiency. This algorithm iteratively calculates the correspondence and the rigid transformation $\mathbf{R}$ and $\vec{t}$ until the objective function converges to a local minimum. In the kth iteration $(k \geq 1)$, two steps are included to conduct the algorithm:

Firstly, set up correspondence between two point sets:

$$c_k(i) = \underset{c(i)\in\{1,2,\ldots,N_y\}}{arg\min} \| \left(\mathbf{R}_{k-1}\vec{x}_i + \vec{t}_{k-1}\right) - \vec{y}_{c(i)}\|_2^2 \text{ for } i = 1, \ldots, N_x, \quad (2)$$

where $\mathbf{R}_{k-1}$ and $\vec{t}_{k-1}$ are the known transformation of the $(k-1)$th iteration.

Secondly, compute the new rotation matrix and translation vector by minimizing squared distance:

$$\left(\mathbf{R}_k, \vec{t}_k\right) = \underset{\mathbf{R}^T\mathbf{R}=\mathbf{I}_n, det(\mathbf{R})=1, \vec{t}}{arg\min} \sum_{i=1}^{N_x} \| \mathbf{R}\vec{x}_i + \vec{t} - \vec{y}_{c_k(i)}\|_2^2 \quad (3)$$

The ICP algorithm runs iteratively until the registration error is small enough or k reaches the maximum number of iterations. The ICP algorithm is fast but it is easily to fall into a local minimum. Moreover, it cannot deal with noises and outliers, either.

2.2. Correntropy

In recent years, correntropy has been proposed in information theoretic learning (ITL) [24]. It is derived from the generalized correlation function of random processes and is directly related to the information potential (IP) of Renyi's quadratic entropy, where the Parzen windowing method is used to estimate the probability distribution of data. Similar to mean square error (MSE), the correntropy can be viewed as a generalized similarity measure between two arbitrary random variables. In this section, we briefly introduce the definition of correntropy and present some of its most important properties.

A general form of correntropy between two arbitrary scalar random variables A and B is defined as follows:

$$V_\sigma(A, B) = \mathrm{E}[\kappa_\sigma(A - B)], \quad (4)$$

where $\kappa_\sigma(\cdot)$ is a symmetric positive kernel function, σ is the kernel width and $E(\cdot)$ represents the mathematical expectation. The kernel bandwidth controls the "window" in which similarity is assessed and the kernel function maps the input space to a higher dimensional space. For simplicity, in the following part we will consider only the Gaussian Kernel:

$$\kappa_\sigma(A - B) = \frac{1}{\sqrt{2\pi}\sigma} \exp\left(-\frac{(A-B)^2}{2\sigma^2}\right). \quad (5)$$

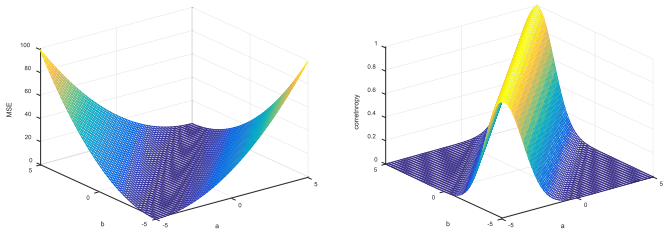

Fig. 1. The distance in the joint space of A and B. (a) MSE. (b) Correntropy.

In practice, the joint probability density function is unknown and only a finite number of data $\{(a_i, b_i)\}_{i=1}^N$ are available, so the sample estimator of correntropy is defined as follows:

$$\hat{V}_{N,\sigma}(A, B) = \frac{1}{N}\sum_{i=1}^{N} \frac{1}{\sqrt{2\pi}\sigma} \exp\left(-\frac{(a_i - b_i)^2}{2\sigma^2}\right) \quad (6)$$

Here we present three properties of correntropy which are important to this paper, without any proving [25].

Property 1: Correntropy is symmetric: $V(A, B) = V(B, A)$.

Property 2: Correntropy is positive and bounded, that's to say, $0 < V_\sigma(A, B) \leq \frac{1}{\sqrt{2\pi}\sigma}$. It reaches its maximum if and only if $A = B$.

Property 3: Correntropy involves all the even moments of the difference between A and B:

$$V_\sigma(A, B) = \frac{1}{\sqrt{2\pi}\sigma}\sum_{n=0}^{\infty} \frac{(-1)^n}{2^n n!} \mathrm{E}\left[\frac{(A-B)^{2n}}{\sigma^{2n}}\right] \quad (7)$$

3. Our algorithm

3.1. Problem statement

It is known that the traditional ICP algorithm performs accurately and efficiently in handling rigid registration, but it could not deal with point set registration with the noises and outliers well. To solve this problem efficiently, the correntropy is incorporated to the point set registration problem for its good property of outlier rejection.

Correntropy is suitable for quantifying the similarity of two random variables A and B. One of the most popular methods is MSE (mean square error), it can be expressed as $\mathrm{MSE}(A, B) = E[(A-B)^2]$ .The distance of A and B in the joint space is shown in Fig. 1. Compared with correntropy, MSE is a quadratic function in the joint space with its minimum along the $a = b$ line like a valley floor. For points far from the bottom, its values increase quadratically with respect to $(a - b)$, which means those noises and outliers in A and B will have a greater impact on the overall MSE. Therefore, MSE works well with data that obeys normal distribution, but if there are many outliers, MSE cannot be a good similarity estimator.

However, correntropy performs much better on this situation. As shown in Fig. 1(b), correntropy also get its maximum along the line $a = b$, for points away from this line, the values decrease rapidly but with a limitation 0. This means when using correntropy as a similarity judgment, this method concerns more about the data nearby the line $a = b$,which bring advantages in non-Gaussian and nonlinear signal processing.

In order to further understand the properties of correntropy, consider the Taylor series expansion shown in Eq. (7). As we can see, correntropy can be viewed as a generalized correlation function between two random variables, which includes all of the even-order terms of the error. Therefore, correntropy also quantifies the higher order terms of the probability distribution function (PDF) within a small neighborhood defined by the kernel width σ.

Please cite this article as: S. Du et al., Robust rigid registration algorithm based on pointwise correspondence and correntropy, Pattern Recognition Letters (2018), https://doi.org/10.1016/j.patrec.2018.06.028

Thus, correntropy has great advantages in processing signals with impulsive noises and outliers, especially compared to second order measurement.

Assume there are two point sets in $\mathbb{R}^n$, a data set $X \triangleq \{\vec{x}_i\}_{i=1}^{N_x} (N_x \in \mathbb{N})$ and a target set $Y \triangleq \{\vec{y}_i\}_{i=1}^{N_y} (N_y \in \mathbb{N})$. The goal of rigid registration is to find a rotation matrix $\mathbf{R}$ and a translation vector $\vec{t}$, with which the data set X can be in the best alignment with the target set Y. Different from the problem stated above, there are lots of noises and outliers in the data set X, in which case the traditional ICP algorithm may suffer a large probability to fail.

The correntropy between two point sets X and Y can be defined as follows:

$$V(\mathrm{X},\mathrm{Y}) = \sum_{i=1}^{N_x} \exp(-||\vec{x}_i - \vec{y}_{c(i)}||_2^2/(2\sigma^2)), \tag{8}$$

where $\vec{y}_{c(i)}$ matches $\vec{x}_i$, and σ is a free parameter which controls the "window size".

Since the data set X undergoes a rigid transformation to align with the target set Y, which means there is a transformation function $T(\vec{x}_i) = \mathbf{R}\vec{x}_i + \vec{t}$ applied on X, so Eq. (8) can be rewritten as:

$$V(\mathrm{X},\mathrm{Y}) = \sum_{i=1}^{N_x} \exp(-||(\mathbf{R}\vec{x}_i + \vec{t}) - \vec{y}_{c(i)}||_2^2/(2\sigma^2)). \tag{9}$$

To simplify Eq. (9), we denote $w(i) = ||\mathbf{R}\vec{x}_i + \vec{t} - \vec{y}_{(i)}||_2^2/(2\sigma^2)$, so the correntropy between two point sets X and Y can be rewritten as $V(X,Y) = \sum_{i=1}^{N_x} \exp(-w(i))$.

In (9), if the data set X can align with the target set Y perfectly, which means there is a small distance between x_i and $\vec{y}_{c(i)}$. In this way, $w(i)$ is very small with a limitation of 0 and $e^{-w(i)}$ is large but no more than 1. If the registration is failed, $w(i)$ is much large and $e^{-w(i)}$ is approximately equal to 0. Taking these properties into consideration, the correntropy is qualified to play a role as the energy function in rigid point set registration. On the other hand, suppose there are some outliers or noises x_j in data set X, and there are no specific points in data set Y which can align with those noises, so $w(j)$ will be larger than those that can be correctly registered, so the correntropy is smaller as well. This means that in the process of point registration, the noises and outliers will be assigned to lower weights while the matched point-pairs will be assigned to higher weights. It means that the impact caused by noises and outliers can be decreased or even be ignored and ideal points can lead the registration to a good result.

Therefore, the new energy function based on the correntropy between the correspondence is shown as follows:

$$E_\sigma(x_i, y_i) = \exp(-||(\mathbf{R}\vec{x}_i + \vec{t}) - \vec{y}_{c(i)}||_2^2/(2\sigma^2)), \tag{10}$$

where $\mathbf{R}$ is the rotation matrix, $\vec{t}$ is the translation vector, $\vec{y}_{c(i)}$ denotes the point in the target set Y corresponds with the point $\vec{x}_i$ in the data set X and σ is a free parameter.

Taking the properties of negative exponential function into consideration, to minimize the error of registration, the objective function should maximize the correntropy, which is shown as follows:

$$\max_{\mathbf{R},\vec{t},c(i)\in\{1,2,\ldots,N_y\}} \sum_{i=1}^{N_x} \exp(-||\mathbf{R}\vec{x}_i + \vec{t} - \vec{y}_{c(i)}||_2^2/(2\sigma)) \tag{11}$$
$$s.t. \quad \mathbf{R}^T\mathbf{R} = \mathbf{I}_m, \det(\mathbf{R}) = 1.$$

3.2. The ICP algorithm based on correntropy

As the objective function (11) is similar to the function (1), we can use the similar algorithm to the ICP algorithm, which includes two steps in each iteration.

Step 1. Assume the $(k-1)$th rigid transformation is known, we can set up the kth correspondence between two point sets:

$$c_k(i) = \underset{c(i)\in\{1,2,\ldots,N_y\}}{\arg\min} (||(\mathbf{R}_{k-1}\vec{x}_i + \vec{t}_{k-1}) - \vec{m}_{c(i)}||_2^2) \text{ for } i = 1, \ldots, N_x \tag{12}$$

Step 2. Compute the kth rigid transformation according to the kth correspondence between two point sets. The goal of our algorithm is to find the rotation matrix $\mathbf{R}$ and translation vector $\vec{t}$, which is shown as follows:

$$(\mathbf{R}, \vec{t}) = \underset{\substack{\mathbf{R}^T\mathbf{R}=\mathbf{I}_m \\ \det(\mathbf{R})=1,\vec{t}}}{\arg\max} \sum_{i=1}^{N_x} \exp\left(-\frac{||\mathbf{R}\vec{x}_i + \vec{t} - \vec{y}_{c(i)}||_2^2}{2\sigma^2}\right) \tag{13}$$

The algorithm repeats until the registration error converges or k reaches the maximum number of iterations.

Step 1 of our algorithm can be solved by many methods such as k – d tree [26,27] or the nearest point search based on Delaunay tessellation [27]. Therefore, Step 2 is the key step for this new algorithm, which will be solved in the next section.

This new ICP algorithm based on correntropy works similar to the traditional ICP algorithm, which means that our algorithm can be proved to be converge monotonically to a local maximum from any given initial values.

3.3. Solve the rigid transformation

In this section, we will compute the rigid transformation $\mathbf{R}$ and $\vec{t}$ in the Step 2 of our algorithm, and then give a closed-form solution.

Taking the derivative of (13) with respect to $\vec{t}$, we can get:

$$\begin{aligned} F(t) &= \frac{\partial \sum_{i=1}^{N_x} e^{-w(i)}}{\partial \vec{t}} \\ &= \sum_{i=1}^{N_x} \left(-\frac{\mathbf{R}\vec{x}_i + \vec{t} - \vec{y}_{c_k(i)}}{\sigma^2} exp\left(-\frac{||\mathbf{R}\vec{x}_i + \vec{t} - \vec{y}_{c_k(i)}||_2^2}{2\sigma^2}\right)\right) \end{aligned} \tag{14}$$

To get an approximate result of $\vec{t}_k$, we set the exponential term to be a known value in (14). In the iterative step, when changing the rigid transformation, the exponential term varies a little. Specifically, we substitute $\mathbf{R}_{k-1}$ into $\mathbf{R}$ and $\vec{t}_{k-1}$ into $\vec{t}$ in exponential term, which is expressed as follows:

$$p_k(i) = \exp\left(-\frac{||\mathbf{R}_{k-1}\vec{x}_i + \vec{t}_{k-1} - \vec{y}_{c_k(i)}||_2^2}{2\sigma^2}\right) \tag{15}$$

Let $F(\vec{t}) = 0$, we can get:

$$\vec{t}_k = \left(\sum_{i=1}^{N_x} (\vec{y}_{c_k(i)} - \mathbf{R}\vec{x}_i) p_k(i)\right) \Big/ \sum_{i=1}^{N} p_k(i) \tag{16}$$

From Eq. (16), to obtain the approximate result of $\vec{t}_k$, we need to compute the rotation $\mathbf{R}_k$. The detailed derivation of $\mathbf{R}_k$ is shown in the following.

Substituting $\vec{t}$ in the energy function (13) with (16), we can obtain the following objective function:

$$\begin{aligned} \mathbf{R}_k = \underset{\mathbf{R}^T\mathbf{R}=\mathbf{I}_n, \det(\mathbf{R})=1}{\arg\max} \sum_{i=1}^{N_x} \exp\Bigg(&- ||(\mathbf{R}\Bigg(\vec{x}_i - \frac{\sum_{i=1}^{N_x} \vec{x}_i p_k(i)}{\sum_{i=1}^{N_x} p_k(i)}\Bigg) \\ &- \Bigg(y_{c_k(i)} - \frac{\sum_{i=1}^{N_x} \vec{y}_{c_k(i)} p_k(i)}{\sum_{i=1}^{N_x} p_k(i)}\Bigg)||_2^2/(2\sigma^2)\Bigg) \end{aligned} \tag{17}$$

We define $\vec{q}_i \triangleq \vec{x}_i - (\sum_{i=1}^{N_x} p_k(i)\vec{x}_i)/\sum_{i=1}^{N_x} p_k(i)$ and $\vec{m}_i \triangleq \vec{y}_{c_k(i)} - (\sum_{i=1}^{N} p_k(i)\vec{y}_{c_k(i)})/\sum_{i=1}^{N} p_k(i)$, Eq. (17) can be simplified as:

$$\mathbf{R}_k = \underset{\mathbf{R}^T\mathbf{R}=\mathbf{I}_n, \det(\mathbf{R})=1}{\arg\max} \sum_{i=1}^{N_x} \exp(-||\mathbf{R}\vec{p}_i - \vec{q}_i||_2^2/(2\sigma^2)) \tag{18}$$

Consider $\mathbf{Q}$ and $\mathbf{M}$ as $N_x \times n$ matrices where each row represents a point $\vec{q}_i$ and $\vec{m}_i$. Then the objective function (18) can be rewritten as:

$$\mathbf{R}_k = \underset{\mathbf{R}^T\mathbf{R}=\mathbf{I}_n, \det(\mathbf{R})=1}{\arg\max} \mathbf{1}_N^T G(\mathbf{M} - \mathbf{Q}\mathbf{R}^T), \tag{19}$$

where $G(\mathbf{M} - \mathbf{Q}\mathbf{R}^T) = \vec{g}$ is a column vector, in which each row $G_i = \exp(-||\mathbf{R}\vec{q}_i - \vec{m}_i||_2^2/(2\sigma^2))$, and $1_{N_x}^T$ is a $1 \times N_x$ vector with each element equals 1.

To solve the constrained optimization problem, we introduce Lagrange multiplier method. Here we define the Lagrange equation as:

$$L(\mathbf{R}, \mathbf{K}, \eta) = 1_{N_x}^T G(\mathbf{M} - \mathbf{Q}\mathbf{R}^T) + tr(\mathbf{K}(\mathbf{R}^T\mathbf{R} - \mathbf{I}_n)) + \eta(\det(\mathbf{R}) - 1) \tag{20}$$

where $\mathbf{K}$ is a $n \times n$ matrix and η is a scalar, both of which serve as the Lagrange multipliers. The symbol tr represents the trace of the matrix.

Taking the partial guidance with **R, K** and η respectively, we can get the following equations:

$$\frac{\partial L}{\partial \mathbf{R}} = -\frac{1}{\sigma^2}(\mathbf{P}^T D(\vec{g})\mathbf{P}\mathbf{R} - \mathbf{P}^T D(\vec{g})\mathbf{Q}) + 2\mathbf{K}\mathbf{R} + \eta\mathbf{R} = \mathbf{0}, \tag{21}$$

$$\frac{\partial L}{\partial \mathbf{K}} = \mathbf{R}^T\mathbf{R} - \mathbf{I}_n = \mathbf{0}, \tag{22}$$

$$\frac{\partial L}{\partial \eta} = \det(\mathbf{R}) - 1 = 0, \tag{23}$$

where $D(\vec{g})$ is the diagonal matrix $diag(\vec{g})$.

The $\vec{g}$ in Eq. (21) can be determined by the last iterative step. Similar with the process of solving $\vec{t}_k$, the result of $\mathbf{R}$ is not a closed-form solution but an approximate solution obtained from a fixed point iterative algorithm. According to Chen et al. [28], this method can eventually converge.

Define $\mathbf{L}' = -\frac{1}{\sigma^2}\mathbf{P}^T D(\vec{\mathbf{g}})\mathbf{P} + 2\mathbf{K} + \eta$, from Eq. (21), we get:

$$\mathbf{L}'\mathbf{R} = -\frac{1}{\sigma^2}\mathbf{P}^T D(\vec{g})\mathbf{Q} \tag{24}$$

Apply SVD algorithm [29] to $\mathbf{L}'\mathbf{R}$, we get

$$\mathbf{L}'\mathbf{R} = \mathbf{U}\mathbf{\Lambda}\mathbf{V}^T \tag{25}$$

where $\mathbf{U}$ and $\mathbf{V}$ is the $n \times n$ unitary matrix, $\mathbf{\Lambda}$ is a $n \times n$ diagonal matrix with each element λ_i non-negative.

Transpose both sides of Eq. (25), it becomes:

$$\mathbf{R}^T\mathbf{L}'^T = -\frac{1}{\sigma^2}(\mathbf{P}^T D(\vec{g})\mathbf{Q})^T = \mathbf{V}\mathbf{\Lambda}\mathbf{U}^T \tag{26}$$

According to Eqs. (25) and (26), it can be gotten that $\mathbf{R}^T\mathbf{L}'^T\mathbf{L}'\mathbf{R} = \mathbf{U}\mathbf{\Lambda}\mathbf{V}^T\mathbf{V}\mathbf{\Lambda}\mathbf{U}^T$. As $\mathbf{R}^T\mathbf{R} = \mathbf{I}_m$, we have:

$$\mathbf{L}'^2 = \mathbf{U}\mathbf{\Lambda}\mathbf{V}^T\mathbf{V}\mathbf{\Lambda}\mathbf{U}^T \tag{27}$$

Besides, it's obvious that $\mathbf{L}'^2\mathbf{L}' = \mathbf{L}'\mathbf{L}'^2$, so $\mathbf{L}'$ can be simplified to a diagonal matrix [30]

$$\mathbf{L}' = \mathbf{U}\mathbf{\Lambda}D(\vec{d})\mathbf{U}^T \tag{28}$$

where $D(\vec{d})$ is the diagonal matrix $diag(\vec{d})$, in which $d_i = 1$ or $d_i = -1$.

In the one hand, from Eq. (28), we have:

$$\det(\mathbf{L}') = \det(\mathbf{U}\mathbf{\Lambda}D(\vec{d})\mathbf{U}^T) = \det(\mathbf{\Lambda})\det(D(\vec{d})) \tag{29}$$

In the other hand, from Eq. (24), we have:

$$\det(\mathbf{L}') = \det(\mathbf{L}')\det(\mathbf{R}) = \det(\mathbf{L}'\mathbf{R}) \tag{30}$$

Considering Eqs. (29) and (30), we get:

$$\det(\mathbf{\Lambda})\det(D(\vec{d})) = \det(\mathbf{L}'\mathbf{R}) \tag{31}$$

Since $\det(\mathbf{\Lambda}) = \lambda_1\lambda_2...\lambda_n \geq 0$, when $\det(\mathbf{L}'\mathbf{R}) > 0$, $\det(D(\vec{d})) = 1$. When $\det(\mathbf{L}'\mathbf{R}) < 0$, $\det(D(\vec{d})) = -1$.

Now we can multiply both sides of Eq. (25) with $\mathbf{L}'^{-1}$, we have:

$$\mathbf{R} = (\mathbf{U}\mathbf{\Lambda}D(\vec{d})\mathbf{U}^T)^{-1}\mathbf{U}\mathbf{\Lambda}\mathbf{V}^T = \mathbf{U}D(\vec{d})^{-1}\mathbf{V}^T \tag{32}$$

From the above, we can obtain an approximate result of rotation matrix $\mathbf{R}_k$ in the kth iteration:

$$\mathbf{R}_k = \mathbf{U}D(\vec{d})^{-1}\mathbf{V}^T \tag{33}$$

where

$$D(\vec{d})^{-1} = \begin{cases} \mathbf{I}_n & \det(\mathbf{P}^T D(\vec{g})\mathbf{Q}) < 0 \\ diag(1, 1, ..., -1) & \det(\mathbf{P}^T D(\vec{g})\mathbf{Q}) > 0 \end{cases} \tag{34}$$

Substitute the result of $\mathbf{R}_k$ into (16), we can get the result of $\vec{t}_k$:

$$\vec{t}_k = \frac{\sum_{i=1}^{N_x}(\vec{y}_{c_k(i)} - \mathbf{R}_k\vec{x}_i)p_k(i)}{\sum_{i=1}^{N_x} p_k(i)} \tag{35}$$

Here we give out a summary of the proposed algorithm (Algorithm 1):

Algorithm 1 The ICP algorithm using correntropy.

Input: A data point set X and a target point set Y
Output: Transformation parameters $\mathbf{R}$ and $\vec{t}$
Initialization: Set the initial rigid transformation parameters $\mathbf{R}_0$ and $\vec{t}_0$, and the iteration step $k = 0$. In addition, set σ in an appropriate way (discussed in Section 4.2).
Do
1) $k = k + 1$.
2) Set up correspondence $\{(i, c_k(i))\}, i = 1, 2, ..., N_x$ via Eq. (12).
3) Compute the rotation matrix $\mathbf{R}_k$ and the translation vector $\vec{t}_k$ via Eqs. (33) and (35) respectively.
4) Update σ for next iteration (discussed in Section 4.2).
Until k reaches the maximum or $|RMS_k - RMS_{k-1}| < \varepsilon$.

4. Theoretical analysis

4.1. Convergence

In this section, the convergence of our algorithm will be proved. The algorithm is similar to the ICP algorithm, and the data point set converges to the target point set by iteration. Although the algorithm cannot guarantee to match the correct point in the target point set Y in one step, the registration can be realized by stepwise approximation. The following theorem will give a more detailed description.

Theorem 1. Under the maximum correntropy criterion, the ICP algorithm based on the correntropy converges to the local maximum from any given initial value.

Proof. Given two point sets $X \triangleq \{\vec{x}_i\}_{i=1}^{N_x}$ and $Y \triangleq \{\vec{y}_i\}_{i=1}^{N_y}$. Suppose that $\mathbf{R}_{k-1}$ and $\vec{t}_{k-1}$ are the $(k-1)$th rotation matrix and translation vector respectively. Define $\vec{p}_{i,k-1} \triangleq \mathbf{R}_{k-1}\vec{x}_i + \vec{t}_{k-1}$, and then $\vec{p}_{i,k-1}$ can find the closest corresponding point $\vec{y}_{c_k(i)}$ in the data set Y. The correntropy between these two point sets is shown as:

$$\varphi_k = \sum_{i=1}^{N_x} \exp(-||\vec{p}_{i,k-1} - \vec{y}_{c_k(i)}||_2^2/(2\sigma^2)) \tag{36}$$

To minimize the registration error between these two point sets, that is, to maximum the correntropy, we can get a best rigid transformation $(\mathbf{R}_k, \vec{t}_k)$, with which X can be registered to Y. Therefore, we have the new correntropy between these two point sets:

$$v_k = \sum_{i=1}^{N_x} \exp(-||\mathbf{R}_k \vec{x}_i + \vec{t}_k - \vec{y}_{c_k(i)}||_2^2/(2\sigma^2)) \tag{37}$$

When the correspondence $c_k(i)$ is determined, we have $N_x \geq v_k \geq \varphi_k$ because $(\mathbf{R}_k, \vec{t}_k)$ is the optimum results of Eq. (13).

In addition, define $\vec{p}_{i,k} \triangleq \mathbf{R}_k \vec{x}_i + \vec{t}_k$, we can find a new corresponding point $\vec{y}_{c_{k+1}(i)}$ by the same method. Now we get the new correntropy between these two point sets:

$$\varphi_{k+1} = \sum_{i=1}^{N_x} \exp(-||\vec{p}_{i,k} - \vec{y}_{c_{k+1}(i)}||_2^2/(2\sigma^2)) \tag{38}$$

Since the new correspondence is gotten from Eq. (12), we have $||\vec{p}_{i,k} - \vec{y}_{c_{k+1}(i)}||_2^2 \leq ||\mathbf{R}_k \vec{x}_i + \vec{t}_k - \vec{y}_{c_k(i)}||_2^2$, that is, $N_x \geq \varphi_{k+1} \geq v_k$

Repeat the above steps, we can get:

$$N_x \geq \cdots \geq v_{k+1} \geq \varphi_{k+1} \geq v_k \geq \varphi_k \geq \cdots \geq v_1 \geq \varphi_1 \geq 0 \tag{39}$$

According to the Monotonic Sequence Theorem "Every bounded monotonic sequence of real numbers is convergent", our algorithm converges to the local maximum from any given initial value.

4.2. Parameter discussion

In correntropy, the kernel size controls the observation window in which similarity is assessed. As a result, the parameter σ influences the ability to resist noises and the accuracy of registration in the proposed algorithm. It is easily to known that if σ is set to a very large number, the proposed algorithm has a similar performance like the ICP algorithm, which means it cannot effectively overcome the influence of noises. On the contrary, if a small σ is given, our algorithm will obtain a satisfying result on noise-resistance, but it is more sensitive to the initial parameters. Moreover, the convergence rate of this algorithm is also influenced by the kernel size σ, that is, a larger σ leads to a faster convergence speed.

To better illustrate the effect of σ on solving the rigid transformation in the proposed algorithm, a simple experiment of point set registration against a wide range of σ is shown in Fig. 2. In this experiment, we choose several different kernel sizes: $\sigma = 100$ as a very large kernel size, $\sigma = 10$ as a middle kernel size, $\sigma = 1$ as a small kernel size, $\sigma_k = \sigma_{k-1} - 0.5$ to show the effect of a liner decay, $\sigma_k = 0.95\sigma_{k-1}$ and $\sigma_k = 0.9\sigma_{k-1}$ to show the effect of exponential decay, where k represents the number of iteration and the initial value of σ is 50. In addition, we also add ICP algorithm in the experiment to compare the performance.

The experiment uses the apple shapes, which are shown in Fig. 2. In the figure, the data set is rotated with four different angles 5, 10, 20 and 30° to demonstrate the effect of different σ on different levels of registration difficulty.

To estimate the registration accuracy, $\varepsilon_{\mathbf{R}}$, the error of rotation matrix is introduced in which $\varepsilon_{\mathbf{R}} = \det(\mathbf{R} - \mathbf{R}_{GT})$, where $\mathbf{R}$ is rotation matrix computed by the algorithm and $\mathbf{R}_{GT}$ is the ground truth. Note that the error of the objective function (3) and (13) which converges to a local extremum, but the error of $\mathbf{R}$ is quite different with above, which may bounce back after reach a local minima.

From the compared results, a larger σ leads to a faster convergence speed at first, but in the last, it cannot converge to a good result, which performs just like ICP algorithm as mentioned above, but a smaller σ requires a longer time to converge. If σ is too small, the algorithm cannot converge to a satisfying result because most of the points are considered as outliers. Moreover, in most cases, an exponential decay performs more stable and faster than a liner decay.

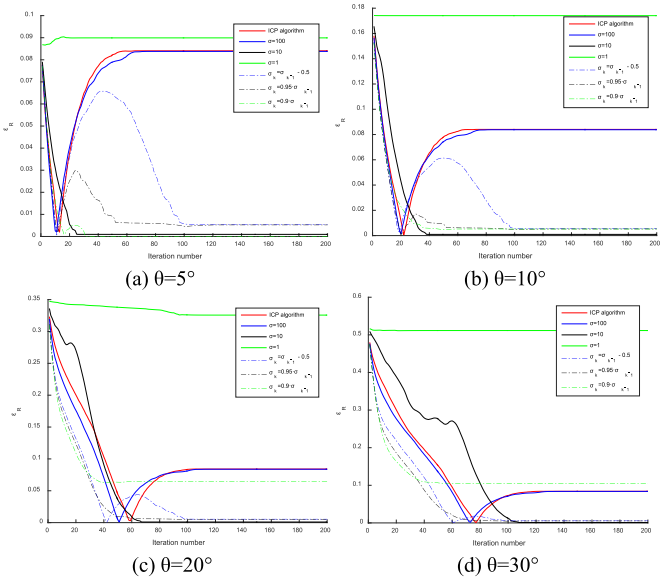

Fig. 2. The effect of kernel size σ on the registration accuracy and convergence rate for different rotations.

Based on observations, the best approach is to change σ during iteration. Firstly start the algorithm with a relatively large σ for a rapid convergence speed, and then anneal σ with an appropriate parameter. There are three advantages of this approach: 1) the algorithm is less prone to being stuck in local extremum; 2) the convergence speed is faster; 3) the accuracy of registration is much higher.

In addition, σ is related to the distribution density of the point sets. Dense point sets need a small σ and sparse point sets need a large σ to ensure the convergences. In this paper, we estimate the point set density firstly, where we sample 200 points in the point cloud and calculate the median D_a of the distances from these points to their nearest neighbors. Secondly, we use 10–30 times D_a as the initial value of σ, and a decay rate 0.96–0.99 is used to anneal σ in each iteration.

5. Experimental results

To check the convergence and robustness of our method, experiments are done based on part B of CE-Shape-1 [31] and The Stanford 3D Scanning Repository [32]. In addition, our algorithm is compared with the traditional ICP algorithm, and they are implemented by MATLAB and run on PC with Intel Core i7-6700 3.4 GHz CPU and 16GB RAM.

5.1. 2D simulations

For the original two-dimensional image data in the dataset, we will first handle these images with cutting, blurring, rotation and translation to simulate the cases of outliers and noisy data, and then extract the edge of the images with the Sobel operator to form the point sets for the experiments.

In this section, the data set part B of CE-Shape-1 [30] are used to demonstrate the accuracy and robustness of the proposed algorithm. In the following, we conduct three different experiments for various cases. In the first experiment, a guitar is cut into two different sets, where only some part is overlapped. In the second experiment, part of the crown is wiped and 10% Gaussian noise is

Table 1
The comparison between the experimental result and the ground truth.

Point-set	Angle		10°	20°	30°
Guitar	ICP	$\varepsilon_{\mathbf{R}}$	0.0827	0.4795	0.4795
		$\varepsilon_{\vec{t}}$	218.4006	272.5416	272.5093
		Time (s)	6.3612	3.1409	2.1962
	Proposed algorithm	$\varepsilon_{\mathbf{R}}$	0.0010	0.0010	1.1967e-04
		$\varepsilon_{\vec{t}}$	1.9537	1.9537	0.0654
		Time (s)	1.0523	1.1322	1.0587
Crown	ICP	$\varepsilon_{\mathbf{R}}$	0.1165	0.2263	0.1593
		$\varepsilon_{\vec{t}}$	11.8867	17.6530	14.0018
		Time (s)	0.1999	0.3260	0.1686
	Proposed algorithm	$\varepsilon_{\mathbf{R}}$	0.0013	0.0022	9.4683e-04
		$\varepsilon_{\vec{t}}$	0.1198	0.1443	0.0753
		Time (s)	0.4515	0.4423	0.28013
Camel	ICP	$\varepsilon_{\mathbf{R}}$	0.0061	0.0120	0.0681
		$\varepsilon_{\vec{t}}$	1.6297	4.2292	14.5127
		Time (s)	0.3757	0.3279	0.2469
	Proposed algorithm	$\varepsilon_{\mathbf{R}}$	6.5881e-04	0.0011	0.0021
		$\varepsilon_{\vec{t}}$	0.4477	0.2475	0.5346
		Time (s)	1.5264	1.0660	1.0411

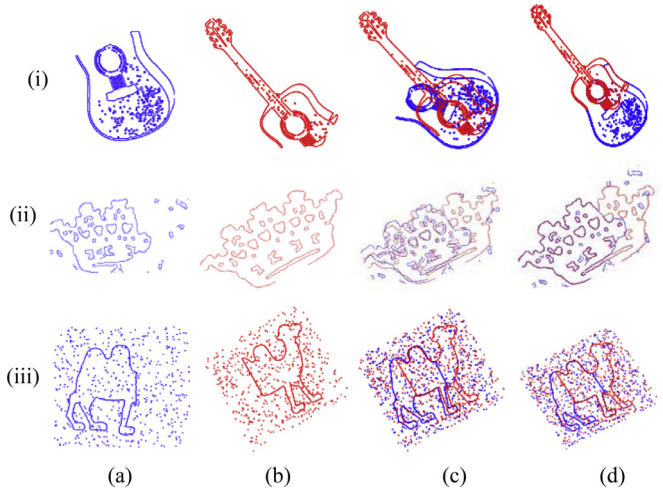

Fig. 3. Compared results of our algorithm and the ICP algorithm with simulated data. (a) The data sets. (b) The target sets. (c) The results of traditional ICP algorithm. (d) The results of our algorithm.

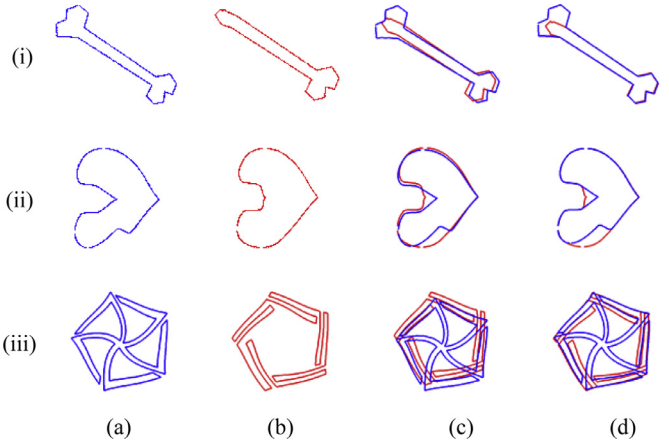

Fig. 4. Compared results of our algorithm and the ICP algorithm with real data. (a) The data sets. (b) The target sets. (c) The results of traditional ICP algorithm. (d) The results of our algorithm.

added to the left part. In the third experiment, a camel is divided into two parts and 1% salt and pepper noises are added to both parts. After that, a rigid transformation is applied to the above different images. We rotate the data with the angle 10°, 20° and 30° respectively and translate with a random value in the interval (0,5). Here we note the initial rotation matrix as $\mathbf{R}_0$ and translation vector $\vec{t}_0$. In addition, since both ICP algorithm and the proposed algorithm converge to local extrema, an initial value is assigned to these two algorithms. Some compared results are shown in Fig. 3.

In Fig. 3, it is easy to find that both our algorithm and traditional ICP algorithm can finish the rigid registration for the last two experiments, while our algorithm gets better results. In the first experiment, the proposed algorithm finishes the registration with a satisfying result while the traditional ICP algorithm fails.

To compare the registration accuracy and efficiency of these two algorithms, we define $\varepsilon_{\mathbf{R}} = ||\mathbf{R} - \mathbf{R}_0||_2$ and $\varepsilon_{\vec{t}} = ||\vec{t} - \vec{t}_0||_2$. All the results are displayed in Table 1.

From Table 1, we can see that whatever condition changes, our algorithm gets smaller errors after the registration, as well as a competitive result on time consuming, which demonstrates the robustness of the proposed algorithm in rigid registration problem with outliers and noises.

5.2. 2D real data experiments

In this section, we choose several couples of original images in the data set part B of CE-Shape-1 [31] for experiments. Here we choose 3 pairs of similar images as the data set and target set. The comparison results are shown in Fig. 4.

From the experimental results, we can see that traditional ICP algorithm could not complete all point set registration, as it fails to register the start and heart data sets. However, on the other hand, our algorithm works well in dealing with all these three data sets, which demonstrates the robustness of our algorithm again.

Note that we don't know the ground truth of the transformation parameters and using RMS as the accuracy judgment of the registration result is obvious unfair because the traditional ICP algorithm naively minimize the RMS error in the registration process. Therefore, we cannot compare the registration error here.

5.3. 3D simulations

This section chooses a 3D point set in The Stanford 3D Scanning Repository [31] to do the simulation experiment for verifying the accuracy and robustness when handling 3D data. In this section, the original 3D point set will be cut and rotated to obtain a new set of data points to simulate the actual situation of abnormal

Please cite this article as: S. Du et al., Robust rigid registration algorithm based on pointwise correspondence and correntropy, Pattern Recognition Letters (2018), https://doi.org/10.1016/j.patrec.2018.06.028

Table 2
The comparison between the experimental result and the ground truth.

Rotation angle (radian)	Registration error	ICP algorithm	Proposed algorithm
[pi/3,0,0]	$\varepsilon_{\mathbf{R}}$	1.7496	1.7333
	$\varepsilon_{\vec{t}}$	5.238e-3	4.391 e−04
[pi/3,pi/3,0]	$\varepsilon_{\mathbf{R}}$	1.9325	1.9842
	$\varepsilon_{\vec{t}}$	0.1880	5.7737e−04
[pi/3, pi/3, pi/3]	$\varepsilon_{\mathbf{R}}$	1.9604	1.9592
	$\varepsilon_{\vec{t}}$	0.0190	5.7701e−04

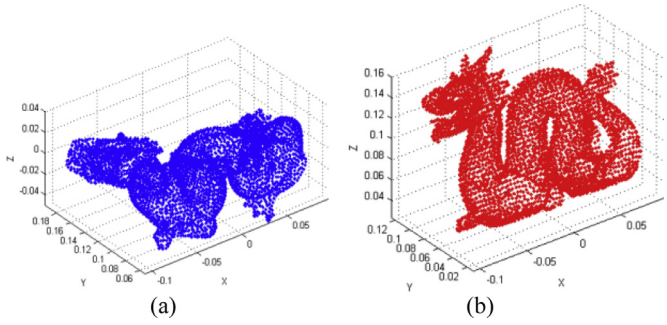

Fig. 5. Simulated data of Dragon. (a) The data set. (b) The target set.

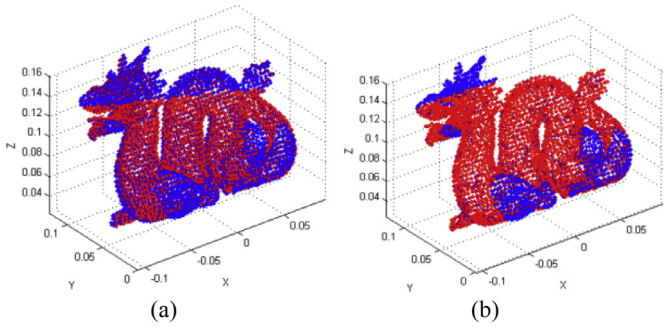

Fig. 6. The compared results. (a) The result of ICP algorithm. (b) The result of proposed algorithm.

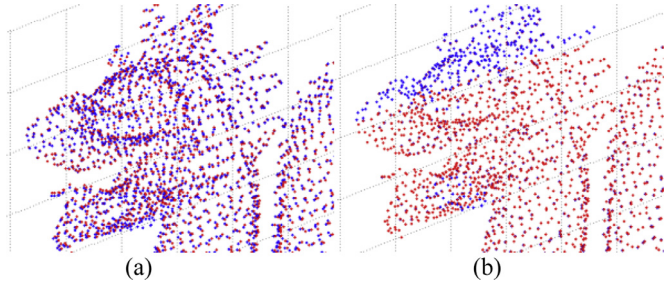

Fig. 7. Enlarged local details. (a) The result of ICP algorithm. (b) The result of proposed algorithm.

points or noises. Finally, the compared results are computed by ICP algorithm and the proposed algorithm respectively.

Fig. 5 shows the data set and the target set respectively. Fig. 6 shows the compared registration results of these two algorithms. It's obvious that the proposed algorithm gets a better registration result. In addition, from the enlarged result shown in Fig. 7, we can see that the proposed algorithm performs better, where the corresponding points are matched together and placed closely.

Table 2 shows the comparison between the experimental result and the ground truth. In this table, the rotation vector $[\alpha, \beta, \gamma]$ is defined, where the data set rotates α around the x-axis, β around the y-axis, γ around the z-axis, so $\varepsilon_{\mathbf{R}}$ and $\varepsilon_{\vec{t}}$ is defined as

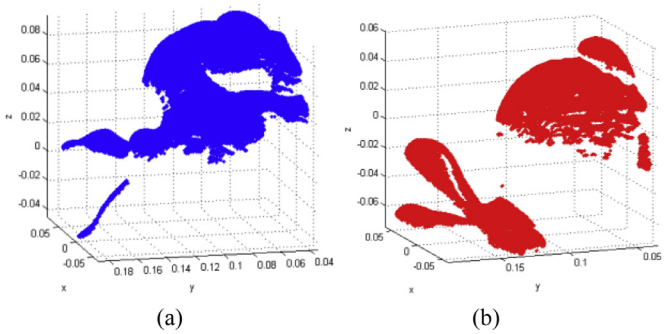

Fig. 8. Bunny data. (a) The data set. (b) The target set.

$\varepsilon_{\mathbf{R}} = ||\mathbf{R} - \mathbf{R}_0||_2$ and $\varepsilon_{\vec{t}} = ||\vec{t} - \vec{t}_0||_2$. As can be seen from the results given in the table, the ICP algorithm based on correntropy proposed in this paper has less error in this experiment, especially the translation vector solved by the proposed algorithm is much better than ICP algorithm, which demonstrates the robustness and accuracy of our algorithm.

5.4. 3D real data experiments

In this section, we choose two partial overlapping data from "Bunny" in The Stanford 3D Scanning Repository [32] to do the experiments. These two point sets are acquired by 3D laser scanner from different viewpoint according to a bunny model, and there are about 40% overlapping part between the model point set and data point set.

In addition to verify the robustness and precision of the ICP algorithm based on correntropy, this experiment is designed to verify the effectiveness of the algorithm in 3D reconstruction applications. In most cases, a particular 3D reconstruction problem can be reduced to be a partial registration problem for two or more point sets. On that condition, the ICP algorithm gives an inaccurate registration result and even fail to match because of the large number of points that cannot match on another point set. However, the proposed algorithm can theoretically be less affected by the outliers, so as to give more accurate registration results.

In order to prevent the local convergence of these two algorithms, the initial value of the rotation matrix between two point sets is given by the rotation information of the scanner. The initial value of the translation vector is automatically calculated from the center of gravity of these two point sets. Fig. 8 shows the two point sets before registration. Figs. 9 and 10 show the comparison of two algorithms. In Fig. 9, although the ICP algorithm can match the general shape of the rabbit in the case of a given initial value, it is clear to see that the overlap ratio of the two point set is not good, especially in the ear and the tail portion of the figure, that is, ICP algorithm cannot precisely complete the registration. However, from Fig. 10, we find that the registration accuracy of our algorithm is much better. This proves once again the robustness and precision of the proposed algorithm and shows its effectiveness in 3D reconstruction.

Please cite this article as: S. Du et al., Robust rigid registration algorithm based on pointwise correspondence and correntropy, Pattern Recognition Letters (2018), https://doi.org/10.1016/j.patrec.2018.06.028

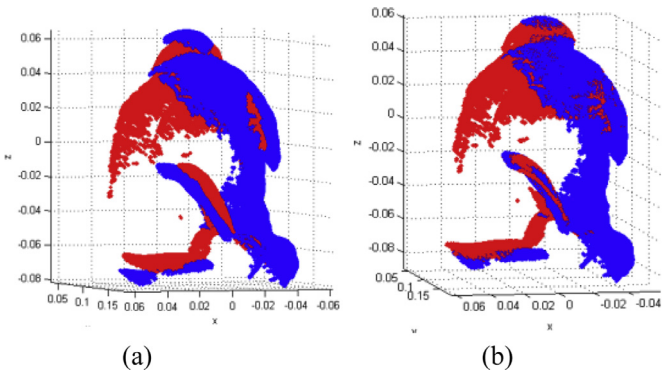

Fig. 9. The compared results. (a) The result of ICP algorithm. (b) The result of proposed algorithm.

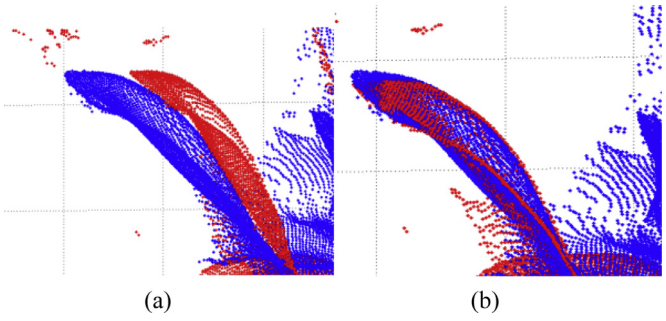

Fig. 10. Enlarged local details. (a) The result of ICP algorithm. (b) The result of proposed algorithm.

6. Conclusion

The ICP algorithm is the most widely used for its fast speed and accuracy in image point set registration field. However, when dealing with the problem of point set with noises or abnormal points, the algorithm is faced with the shortcomings of lack of robustness. In this paper, we propose a new point set registration model based on the idea of correntropy. On this basis, we propose the ICP algorithm based on correntropy, and use singular value decomposition to give the closed-form solution of the transformation at each iterative step of the proposed algorithm. Moreover, the local convergence of the algorithm is proved theoretically. The experimental results on 2D shape data sets and 3D point sets demonstrate that the ICP algorithm based on correntropy is proposed with good accuracy and robustness. In the future, the method will be applied to much more applications, such as normalized samples for machine learning, 3D reconstruction, robot positioning and navigation, biometric identification.

Conflict of interest

The authors declared that they have no conflicts of interest to this work.

Acknowledgments

This work was supported by the National Natural Science Foundation of China under Grant Nos. 61573274 and 61627811, the Fundamental Research Funds for the Central Universities under Grant No. xjj2017005, and the Program of Introducing Talents of Discipline to University under Grant No. B13043.

References

[1] X. Zhu, S. Zhang, R. Hu, Y. Zhu, J. Song, Local and global structure preservation for robust unsupervised spectral feature selection, IEEE Trans. Knowl. Data Eng. 30 (2018) 517–529.
[2] W. Zheng, X. Zhu, Y. Zhu, R. Hu, C. Lei, Dynamic graph learning for spectral feature selection, Multimedia Tools Appl. (2017) 1–17.
[3] C. Lei, X. Zhu, Unsupervised feature selection via local structure learning and sparse learning, Multimedia Tools Appl. (2017) 1–18.
[4] X. Zhao, N. Wang, Y. Zhang, S. Du, Y. Gao, J. Sun, Beyond pairwise matching: person reidentification via high-order relevance learning, IEEE Trans. Neur. Netw. Learn. Syst. (2018).
[5] Y. Gao, R. Ji, P. Cui, Q. Dai, G. Hua, Hyperspectral image classification through bilayer graph-based learning, IEEE Trans. Image Process. 23 (2014) 2769–2778.
[6] D. Wang, S. Du, J. Zhou, J. Xue, Accurate modified normal based ICP for 3D mapping, in: International Conference on Internet Multimedia Computing and Service, 2016, pp. 223–227.
[7] M.W.M.G. Dissanayake, P. Newman, S. Clark, H.F. Durrant-Whyte, A solution to the simultaneous localization and map building (SLAM) problem, IEEE Trans. Robot. Autom. 17 (2001) 229–241.
[8] S. Du, Y. Guo, G. Sanroma, D. Ni, G. Wu, D. Shen, Building dynamic population graph for accurate correspondence detection, Med. Image Anal. 26 (2015) 256.
[9] G.P. Penney, J. Weese, J.A. Little, P. Desmedt, D.L.G. Hill, D.J. Hawkes, A comparison of similarity measures for use in 2D-3D medical image registration, in: International Conference on Medical Image Computing and Computer-Assisted Intervention, 1998, pp. 1153–1161.
[10] Y. Chen, G. Medioni, Object modeling by registration of multiple range images, in: IEEE International Conference on Robotics and Automation, 1991. Proceedings., 1991, IEEE, 1991, pp. 2724–2729.
[11] P.J. Besl, N.D. McKay, Method for registration of 3-D shapes, in: Robotics-DL tentative, International Society for Optics and Photonics, 1992, pp. 586–606.
[12] Z. Zhang, Iterative point matching for registration of free-form curves and surfaces, Int. J. Comput. Vision 13 (1994) 119–152.
[13] A.W. Fitzgibbon, Robust registration of 2D and 3D point sets, Image Vision Comput. 21 (2003) 1145–1153.
[14] S. Granger, X. Pennec, Multi-scale EM-ICP: a fast and robust approach for surface registration, in: Computer Vision—ECCV 2002, 2006, pp. 69–73.
[15] G. Blais, M.D. Levine, Registering Multiview Range Data to Create 3D Computer Objects, IEEE Computer Society, 1995.
[16] D. Chetverikov, D. Svirko, D. Stepanov, P. Krsek, The trimmed iterative closest point algorithm, in: 16th International Conference on Pattern Recognition, 2002. Proceedings., IEEE, 2002, pp. 545–548.
[17] S. Du, J. Liu, C. Zhang, J. Zhu, K. Li, Probability iterative closest point algorithm for m-D point set registration with noise, Neurocomputing 157 (2015) 187–198.
[18] S. Du, J. Liu, B. Bi, J. Zhu, J. Xue, New iterative closest point algorithm for isotropic scaling registration of point sets with noise, J. Visual Commun. Image Represent. 38 (2016) 207–216.
[19] S. Granger, X. Pennec, Multi-scale EM-ICP: a fast and robust approach for surface registration, in: Computer Vision—ECCV 2002, 2006, pp. 69–73.
[20] H. Chui, A. Rangarajan, A new point matching algorithm for non-rigid registration, Comput. Vision Image Understanding 89 (2003) 114–141.
[21] A. Myronenko, X. Song, Point set registration: coherent point drift, IEEE Trans. Pattern Anal. Mach. Intell. 32 (2010) 2262–2275.
[22] E. Hasanbelliu, L. Sanchez Giraldo, J.C. Principe, Information theoretic shape matching, IEEE Trans. Pattern Anal. 36 (2014) 2436–2451.
[23] B. Chen, J. Wang, H. Zhao, N. Zheng, J. Principe, Convergence of a fixed-point algorithm under maximum correntropy criterion, IEEE Signal Processing Letters 22 (10) (2015) 1723–1727.
[24] D. Erdogmus, J.C. Principe, Information Theoretic Learning, Springer, New York, 2010.
[25] W. Liu, P.P. Pokharel, J.C. Principe, Correntropy: properties and applications in non-Gaussian signal processing, IEEE Trans. Signal Process. 55 (2007) 5286–5298.
[26] M. Greenspan, M. Yurick, Approximate k-d tree search for efficient ICP, in: Fourth International Conference on 3-D Digital Imaging and Modeling (3DIM), IEEE, 2003, pp. 442–448.
[27] S. Zhang, X. Li, Z. Ming, X. Zhu, R. Wang, Efficient kNN classification with different numbers of nearest neighbors, IEEE Trans. Neural Netw. Learn. Syst. (2017) 1–12.
[28] B. Chen, J. Wang, H. Zhao, N. Zheng, J.C. Príncipe, Convergence of a fixed-point algorithm under maximum correntropy criterion, IEEE Signal Process. Lett. 22 (2015) 1723–1727.
[29] K. Dan, A singularly valuable decomposition: the SVD of a matrix, College Math. J. 27 (1996) 2–23.
[30] H.L. Chou, W.H. Tsai, A new approach to robot location by house corners, Pattern Recogn. 19 (1986) 439–451.
[31] L.J. Latecki, R. Lakamper, T. Eckhardt, Shape descriptors for non-rigid shapes with a single closed contour, in: Computer Vision and Pattern Recognition, 2000. Proceedings. IEEE Conference on, vol. 1, 2000, pp. 424–429.
[32] M. Levoy, J. Gerth, B. Curless, K. Pull, The Stanford 3D scanning Repository, 2005 URL http://www-graphics.stanford.edu/data/3dscanrep.

Please cite this article as: S. Du et al., Robust rigid registration algorithm based on pointwise correspondence and correntropy, Pattern Recognition Letters (2018), https://doi.org/10.1016/j.patrec.2018.06.028